the lower silicon-ligand bond strengths[42] and greater positive charge at silicon[43] in the pentacoordinated anionic state compared to that in the tetracoordinate state as factors influencing enhanced reactivity of five-coordinated anionic silicon.

Acknowledgment. The support of this research by the National Science Foundation (Grant CHE 88-19152) is gratefully acknowledged.

Supplementary Material Available: Tables of atomic coordinates, thermal parameters, additional bond lengths and angles, and hydrogen atom parameters (Tables S1–S4 for **1** and Tables S5–S8 for **5**, respectively) (22 pages); tables of calculated and observed structure factors (20 pages). Ordering information is given on any current masthead page.

---

(43) Baybutt, P. *Mol. Phys.* **1975**, *29*, 389.

Contribution from the Department of Chemistry,
University of Massachusetts, Amherst, Massachusetts 01003

Boat and Chair Forms for Sulfur-Containing Cyclic Oxyphosphoranes[1,2]

Johannes Hans, Roberta O. Day, Lori Howe,[3] and Robert R. Holmes*

Received December 10, 1990

Oxidative-addition reactions of pentafluorophenol or phenanthrenequinone to cyclic phosphites resulted in the formation of the new cyclic phosphoranes $(Me_2C_3H_4O_2)P(OC_6F_5)_2(S\text{-}Xyl)$ (**1**), $(C_3H_6S_2)P(OC_6F_5)_2(O\text{-}Xyl)$ (**2**), and $(C_2H_4S_2)P(O_2C_{14}H_8)(O\text{-}Xyl)$ (**3**). The monocyclic derivative **1** is unique in having the phosphorinane ring in a chair conformation at axial–equatorial sites of a trigonal bipyramid (TBP). Previously, boat forms were found at this location unless hydrogen bonding was present. Further, the ring in **1** has equal P–O axial and equatorial bond lengths, representing the first observance of this kind in pentacoordinate phosphorus chemistry. A combination of an electronegativity effect ascribed to the pentafluorophenyl groups and a steric contribution in the molecule is suggested as responsible for the uniqueness of **1**. Both **2** and **3** have TBP structures with the thiophosphorinane ring in **2** residing in a twisted-boat conformation and the sulfur-containing five-membered ring of **3** present in an envelope conformation. Both rings are located at axial–equatorial sites. ^1H NMR spectra reveal that **1** undergoes rapid pseudorotation at room temperature involving axial–equatorial ring interchange, which is "stopped" at –65 °C. Most likely **2** is nonrigid similar to **1**. The ^1H NMR spectra of **3** are invariant from 20 to –90 °C, showing nonrigid behavior indicating axial–equatorial to diequatorial activation for the phenanthrene ring in a pseudorotational process allowing equivalence of all four methylene protons of the sulfur-containing five-membered saturated ring. The monocyclic derivative **1** crystallizes in the triclinic space group $P\bar{1}$ with $a = 11.239$ (11) Å, $b = 11.288$ (5) Å, $c = 11.934$ (8) Å, $\alpha = 74.72$ (5)°, $\beta = 65.34$ (6)°, $\gamma = 74.58$ (6)°, and $Z = 2$. The monocyclic derivative **2** crystallizes in the monoclinic space group $P2_1/c$ with $a = 14.485$ (5) Å, $b = 10.573$ (4) Å, $c = 16.626$ (3) Å, $\beta = 99.85$ (2)°, and $Z = 4$. Spirocyclic **3** crystallizes in the monoclinic space group $P2_1/c$ with $a = 13.493$ (2) Å, $b = 9.048$ (3) Å, $c = 18.149$ (6) Å, $\beta = 96.86$ (2)°, and $Z = 4$. The final conventional unweighted residuals are 0.095 (**1**), 0.036 (**2**), and 0.044 (**3**).

Introduction

In our work on oxyphosphoranes with saturated six-membered rings, we reported that the normally observed boat conformation, which resides in axial–equatorial sites of a trigonal bipyramid (TBP), resulted in chair conformations when hydrogen bonding was introduced into the framework.[4] This was found for the spirocyclic tetraoxyaminophosphoranes A–C by X-ray analysis.

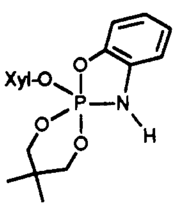

A

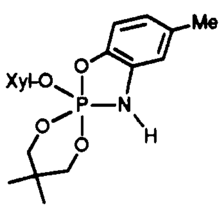

B

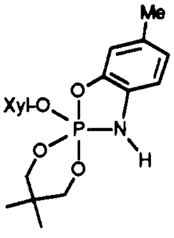

C

For A, the solid-state structure consisted of a spiral arrangement of hydrogen-bonded (N–H- - -O) chains of trigonal bipyramids with the phosphorinane ring in a twist-chair form. For B and C, dimer formulations were found. In these dimer arrangements, both twist-chair and twist-boat forms were present. The results indicate that the conformational conversion of boat and chair forms for phosphorinane rings in oxyphosphoranes is within the range of hydrogen-bond energies, i.e., of the order of a few kilocalories per mole.

Variable-temperature solution ^1H NMR data[4] on A–C indicate intramolecular exchange (pseudorotation) via an intermediate having the phosphorinane ring located diequatorially, e.g., A.

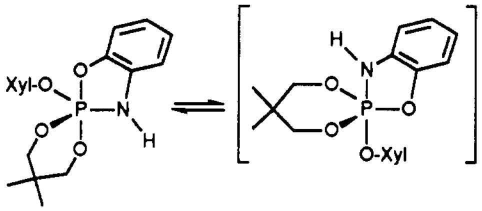

Activation energies suggest that a minimum of about 10 kcal/mol is required to stabilize a six-membered ring of an oxyphosphorane of the type used here in diequatorial positions in preference to the axial–equatorial positions of a TBP when xylyloxy groups are present. However, so far no X-ray analyses of this class of compounds have shown diequatorial ring placement.[4-10]

---

(1) (a) Pentacoordinated Molecules. 88. (b) Part 87: Kumara Swamy, K. C.; Sreelatha, C.; Day, R. O.; Holmes, J. M.; Holmes, R. R. *Inorg. Chem.*, preceding paper in this issue.

(2) Presented in part at the 201st National Meeting of the American Chemical Society, Atlanta, GA, April 1991; INOR 300.

(3) This work represents in part a portion of the M.S. Thesis of Lori Howe, University of Massachusetts, Amherst, MA, 1990.

(4) Day, R. O.; Kumara Swamy, K. C.; Fairchild, L.; Holmes, J. M.; Holmes, R. R. *J. Am. Chem. Soc.* **1991**, *113*, 1627.

(5) Kumara Swamy, K. C.; Burton, S. D.; Holmes, J. M.; Day, R. O.; Holmes, R. R. *Phosphorus, Sulfur, Silicon* **1990**, *53*, 437.

(6) Schomburg, D.; Hacklin, H.; Röschenthaler, G.-V. *Phosphorus Sulfur* **1988**, *35*, 241.

(7) Kumara Swamy, K. C.; Holmes, J. M.; Day, R. O.; Holmes, R. R. *J. Am. Chem. Soc.* **1990**, *112*, 6092 and references cited therein.

(8) Kumara Swamy, K. C.; Day, R. O.; Holmes, J. M.; Holmes, R. R. *J. Am. Chem. Soc.* **1990**, *112*, 6095.

(9) Burton, S. D.; Kumara Swamy, K. C.; Holmes, J. M.; Day, R. O.; Holmes, R. R. *J. Am. Chem. Soc.* **1990**, *112*, 6104.

(10) Holmes, R. R.; Kumara Swamy, K. C.; Holmes, J. M.; Day, R. O. *Inorg. Chem.* **1991**, *30*, 1052.

0020-1669/91/1330-3132$02.50/0

It is important to ascertain what features of oxyphosphoranes containing saturated six-membered rings might induce diequatorial ring placement in a TBP geometry. This class of substances serves as activated-state models for intermediates in a wide variety of nonenzymatic[11-13] as well as enzymatic reactions[14-16] of cyclic phosphates. In *c*-AMP action with protein kinases, diequatorial ring placement has been proposed,[14,15] whereas action with phosphodiesterases has led to phosphorane model intermediates containing axial–equatorial placement of the phosphorinane ring.[15] Thus far, the nearest approach to a possible model intermediate for *c*-AMP action that has been structurally characterized by X-ray analysis are the oxyphosphoranes I[10,17] and II[18] containing trans-fused cyclopentane rings.

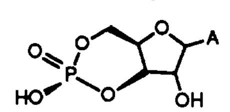

c-AMP

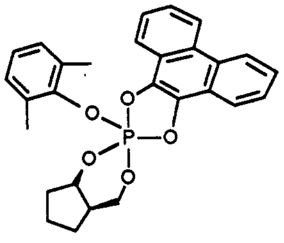

I[10]

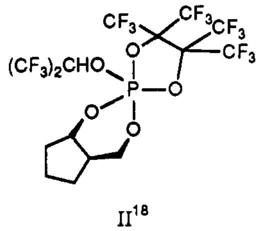

II[18]

In this study, we concentrate on the use of sulfur ligands and the pentafluorophenoxy ligand. The latter has a greater electronegativity requirement compared to the xylyloxy ligand that we have previously employed.[4-10] It is also of interest to examine the use of sulfur in place of ring oxygen atoms to ascertain if any adjustments in conformational or structural preferences would manifest themselves. This resulted in the synthesis, X-ray analysis, and NMR study of the monocyclic phosphoranes **1** and **2** containing pentafluorophenoxy ligands. The spirocyclic phosphorane **3** having a sulfur-containing five-membered-ring system was also synthesized and structurally characterized for comparison with **2** and a previously reported[7] related thiophosphorane possessing a six-membered ring (D).

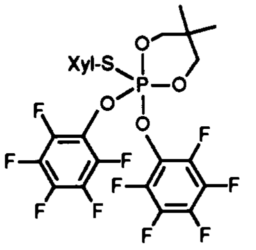

1

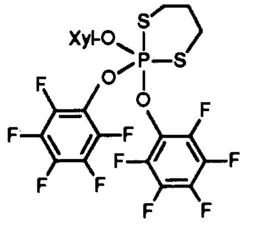

2

Experimental Section

All reactions were carried out by using standard Schlenk techniques in an inert atmosphere of nitrogen. Residual moisture and oxygen in tank nitrogen gas was removed with a train consisting of a phosphorus pentoxide column and a copper catalyst unit. Solvents (Fisher Scientific) were freshly distilled before using. Diethyl ether and tetrahydrofuran were dried over sodium benzophenone by refluxing until a blue color persisted. 1,2-Ethanediol, 1,3-propanedithiol, 9,10-phenanthrenequinone, and 2,6-dimethylphenol were purchased from Aldrich. Pentafluorophenol was obtained from SCM Specialty Chemicals.

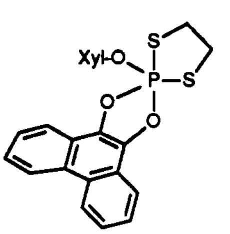

3

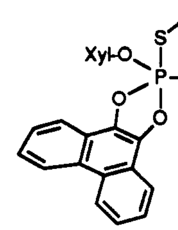

D[7]

^{1}H NMR spectra were recorded on a Varian Associates XL 200 FT-NMR instrument. ^{31}P NMR spectra were recorded on the Varian Associates XL 300 FT-NMR spectrometer. Chemical shifts for ^{31}P NMR spectra were obtained by setting triphenyl phosphate ($CDCl_3$) at −18.0 ppm[19] and are referenced to 85% H_3PO_4 with negative shifts upfield. Spectra were obtained at 23 °C unless otherwise stated.

Syntheses. ((2,2-Dimethyl-1,3-propanediyl)dioxy)(2,6-dimethylthiophenoxy)bis(pentafluorophenoxy)phosphorane, $(Me_2C_3H_4O_2)P(OC_6F_5)_2(S\text{-}Xyl)$ (1). To a stirred solution of 2-(2,6-dimethylthiophenoxy)-5,5-dimethyl-1,3,2-dioxaphosphorinane[10] (1.7 g, 6.0 mmol) and pentafluorophenol (2.3 g, 12.6 mmol) in diethyl ether (150 mL) was added at −78 °C a solution of *N*-chlorodiisopropylamine (0.85 g, 6.0 mmol) in diethyl ether (50 mL). The stirred reaction mixture was allowed to reach room temperature. Stirring was continued for an additional 2 h. The amine hydrochloride was filtered off and the solvent removed under reduced pressure. During concentration, crystallization occurred. The colorless crystals were filtered out, washed with diethyl ether (5 mL), and dried (yield 2.3 g, 57.4%), mp 118–120 °C. Anal. Calcd for $C_{25}H_{19}O_4SF_{10}P$: C, 47.18; H, 3.01. Found: C, 46.69; H, 3.02. ^{1}H NMR ($CDCl_3$, ppm, 20 °C): 0.96 (s, $OCH_2C(CH_3)_2$, 6 H), 2.69 (d, $J = 2.4$ Hz, $SC_6H_3(CH_3)_2$, 6 H), 3.85 (d, $^3J_{P-H} = 17.8$ Hz, OCH_2, 4 H), 7.09 (s, $SC_6H_3(CH_3)_2$, 2 H_m), 7.10 (s, $SC_6H_3(CH_3)_2$, 1 H_p). ^{1}H NMR ($CDCl_3$, ppm, −70 °C): 0.75 (s, $OCH_2C(CH_3)_2$, 3 H), 1.14 (s, $OCH_2C(CH_3)_2$, 3 H), 2.56 (s, $SC_6H_3(CH_3)_2$, 3 H), 2.62 (s, $SC_6H_3(CH_3)_2$, 3 H), 3.4–4.3 (m, OCH_2, 4 H), 7.02 (s, $SC_6H_3(CH_3)_2$, 2 H_m), 7.07 (s, $SC_6H_3(CH_3)_2$, 1 H_p). ^{31}P NMR ($CDCl_3$, ppm): −44.71.

Variable-temperature ^{1}H NMR spectra in CD_2Cl_2 solution were recorded at 200 MHz from −80 to +30 °C. At ≤−10 °C marked broadening of the OCH_2 and $SCH_2C(CH_3)_2$ proton signals occurred ($T_c \sim -10$ °C). At −50 °C splitting of the singlet of the $OC_6H_3(CH_3)_2$ protons took place while the $OC_6H_3(CH_3)_2$ pattern remained intact. ^{1}H NMR spectra in toluene-d_8 also were obtained at 200 MHz over the temperature range of −80 to 16 °C. Patterns and changes with temperature were similar to those observed with $CDCl_3$ ($T_c \sim -10$ °C). However, there were solvent shifts. ^{1}H NMR ($C_6D_5CD_3$, ppm, 16 °C): 0.54 (s, $OCH_2C(CH_3)_2$, 6 H), 2.84 (s, $SC_6H_3(CH_3)_2$, 6 H), 3.52 (d, $^3J_{P-H} = 19.2$ Hz, OCH_2, 4 H), 6.99 (s, $SC_6H_3(CH_3)_2$, 3 H). ^{1}H NMR ($C_6D_5CD_3$, ppm, −60 °C): 0.28 (s, $OCH_2C(CH_3)_2$, 3 H), 0.66 (s, $OCH_2C(CH_3)_2$, 3 H), 2.85 (s, $SC_6H_3(CH_3)_2$, 3 H), 3.10 (s, $SC_6H_3(CH_3)_2$, 3 H), 2.7–4.0 (m, OCH_2, 4 H), 7.00 (s, $SC_6H_3(CH_3)_2$, 3 H).

(1,3-Propanediyldithio)(2,6-dimethylphenoxy)bis(pentafluorophenoxy)phosphorane, $(C_3H_6S_2)P(OC_6F_5)_2(O\text{-}Xyl)$ (2). To a solution of 2-(2,6-dimethylphenoxy)-1,3,2-dithiaphosphorinane[5] (1.3 g, 5.0 mmol) and pentafluorophenol (1.85 g, 10.0 mmol) in diethyl ether (100 mL) was added at −78 °C a solution of *N*-chloroisopropylamine (0.68 g, 5.0 mmol) in diethyl ether (50 mL). The reaction mixture was allowed to reach room temperature and then stirred for an additional 1 h. After filtration and removal of the solvent under reduced pressure, crystallization occurred (yield 1.2 g, 38.2%), mp 112–114 °C. Anal. Calcd for $C_{23}H_{15}F_{10}O_3S_2P$: C, 44.23; H, 2.42. Found: C, 44.48; H, 3.15. ^{1}H NMR ($CDCl_3$, ppm, 20 °C): 1.98 (quin, SCH_2CH_2, $^3J_{H_a-H_b} = 7.0$ Hz, 2 H), 2.38 (s, $OC_6H_3(CH_3)_2$, 6 H), 3.08 (dt, SCH_2, $^3J_{P-SCH_2} = 31$ Hz, $^3J_{H_a-H_b} = 7.0$ Hz, 4 H; H_a refers to the four equivalent protons of the two SCH_2 groups and H_b refers to the two equivalent protons of the single CH_2CH_2 group), 3.12 (m, SCH_2, 2 H), 7.05 (s, $OC_6H_3(CH_3)_2$, 3 H). ^{31}P NMR ($CDCl_3$, ppm): −15.96.

(9,10-Phenanthrenediyldioxy)(2,6-dimethylphenoxy)(1,2-ethylenedithio)phosphorane, $(C_2H_4S_2)P(O_2C_{14}H_8)(O\text{-}Xyl)$ (3). 2-(2,6-Dimethylphenoxy)-1,3,2-dithiaphospholane (4) (3.2 g, 13.1 mmol) and phenanthrenequinone (2.73 g, 13.1 mmol) were heated together at 140 °C for

---

(11) Holmes, R. R. *Pentacoordinated Phosphorus-Reaction Mechanisms*; ACS Monograph No. 176; American Chemical Society: Washington, DC, 1980; Vol. II, Chapter 2 and references cited therein.

(12) Cherkasov, R. A.; Ovchinnickov, V. V.; Pudovik, M. A.; Pudovik, A. N. *Russ. Chem. Rev. (Engl. Transl.)* **1982**, *51*, 746.

(13) Hall, C. R.; Inch, T. D. *Tetrahedron* **1980**, *36*, 2059.

(14) van Ool, P. J. J. M.; Buck, H. M. *Recl. Trav. Chim. Pays-Bas* **1981**, *100*, 79.

(15) van Ool, P. J. J. M.; Buck, H. M. *Eur. J. Biochem.* **1982**, *121*, 329.

(16) Mehdi, S.; Coderre, J. A.; Gerlt, J. A. *Tetrahedron* **1983**, *39*, 3483 and references cited therein.

(17) First reported at the 200th National Meeting of the American Chemical Society, Washington, DC, Aug 1990; INOR 26.

(18) Yu, J. H.; Sopchik, A. E.; Arif, A. M.; Bentrude, W. G. *J. Org. Chem.* **1990**, *55*, 3444.

(19) Emsley, J.; Hall, D. *The Chemistry of Phosphorus*; Wiley: New York, 1976; p 82.

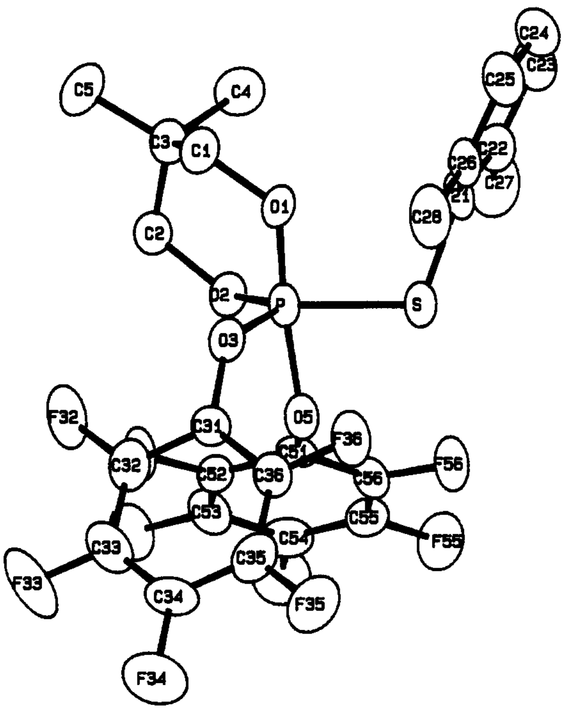

Figure 1. ORTEP plot of $(Me_2C_3H_4O_2)P(OC_6F_5)_2(S\text{-}Xyl)$ (**1**) with thermal ellipsoids at the 30% probability level. Hydrogen atoms are omitted for clarity.

15 min. After the reaction mixture was allowed to reach room temperature, the solidified mass was dissolved in 10 mL of THF and filtered. The solvent was removed under reduced pressure to obtain **3** as a slightly yellow solid (yield 1.37 g, 13.8%). ^1H NMR ($CDCl_3$, ppm, 20 °C): 2.39 (s, $OC_6H_3(CH_3)_2$, 6 H), 3.27 (d, $^3J_{P-H} = 22.1$ Hz, S–CH_2, 4 H), 6.85 (s, br, $OC_6H_3(CH_3)_2$, H_{Ar}, 3 H), 7.52–7.68 (m, H_{Phen} (H2, H3, H6, H7), 4 H), 7.88 (d, H_{Phen} (H1, H8 or H4, H5), 2 H), 8.65 (m, H_{Phen} (H4, H5 or H1, H8), 2 H). ^{31}P NMR ($CDCl_3$, ppm): 25.2.

Other than line shifts, a similar spectrum resulted in toluene-d_8 solution conducted at 200 MHz over the range from −90 to +20 °C. ^1H NMR ($C_6D_5CD_3$, ppm, 20 °C): 2.29 (s, $OC_6H_3(CH_3)_2$, 6 H), 2.53 (d, $^3J_{P-H} = 22.5$ Hz, SCH_2, 4 H), 6.51 (s, $OC_6H_3(CH_3)_2$, 3 H), 7.17 (quin, H_{Phen} (H2, H3, H6, H7), 4 H), 7.81 (d, H_{Phen} (H1, H8 or H4, H5), 2 H), 8.18 (d, H_{Phen} (H4, H5 or H1, H8), 2 H).

The ^1H spectra either in $CDCl_3$ or toluene-d_8 were essentially invariant in pattern and chemical shift over the entire temperature range studied.

2-(2,6-Dimethylphenoxy)-1,3,2-dithiaphospholane, $(C_2H_4S_2)P(O\text{-}Xyl)$ (4). To a solution of 2-chloro-1,3,2-dithiaphospholane[20,21] (14.0 g, 88.3 mmol) (prepared from phosphorus trichloride, ethane-1,2-dithiol, and triethylamine in diethyl ether and purified by distillation in vacuo) and 2,6-dimethylphenol (10.8 g, 88.3 mmol) in diethyl ether (300 mL) was added a solution of triethylamine (8.9 g, 88.3 mmol) in diethyl ether (50 mL) dropwise over a period of 1 h. The solution was stirred for an additional 3 h. The reaction mixture was filtered and the solvent removed by distillation. The residue was dissolved in diethyl ether, and the solution was filtered. The solvent was removed completely to obtain the new compound (**4**) as an oil (yield 18.7 g, 87%). Anal. Calcd for $C_{10}H_{13}OS_2P$: C, 49.15; H, 5.36. Found: C, 49.58; H, 5.19. ^1H NMR ($CDCl_3$, ppm, 20 °C): 2.36 (s, $OC_6H_3(CH_3)_2$, 6 H), 3.30–3.75 (m, SCH_2, 4 H), 6.90–7.10 (m, $OC_6H_3(CH_3)_2$, 3 H). ^{31}P NMR ($CDCl_3$, ppm): 161.12.

X-ray Experimental Section

All X-ray crystallographic studies were done by using an Enraf-Nonius CAD4 diffractometer and graphite-monochromated molybdenum radiation ($\lambda(K\bar{\alpha}) = 0.71073$ Å) at an ambient temperature of 23 ± 2 °C. Details of the experimental procedures have been described previously.[22]

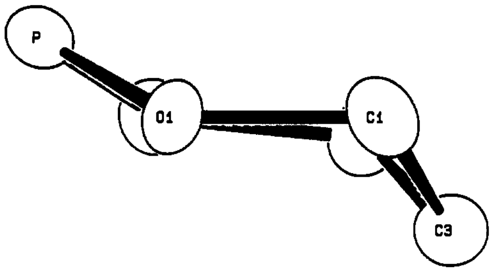

Figure 2. ORTEP plot showing the flattened chair conformation of the six-membered phosphorinane ring in **1**.

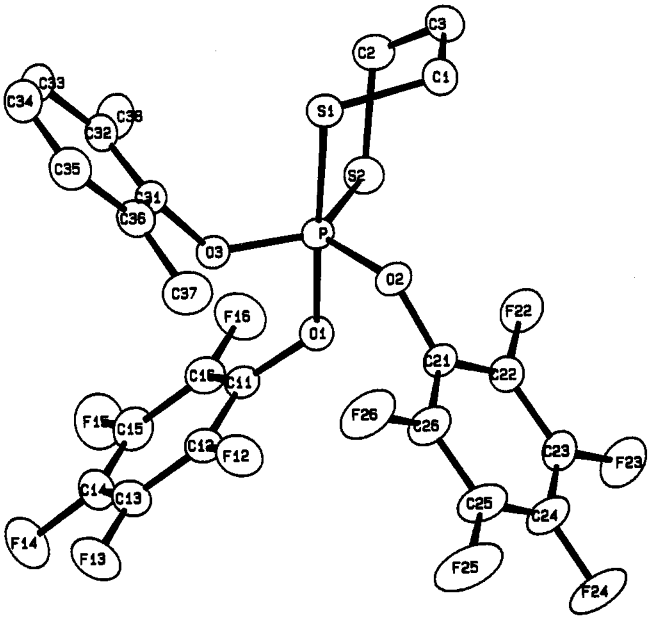

Figure 3. ORTEP plot of $(C_3H_6S_2)P(OC_6F_5)_2(O\text{-}Xyl)$ (**2**) with thermal ellipsoids at the 30% probability level. Hydrogen atoms are omitted for clarity.

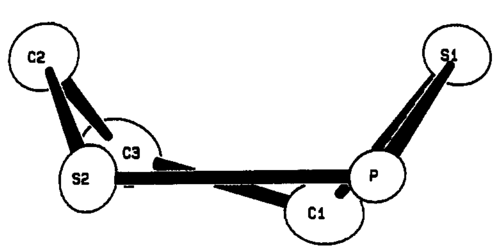

Figure 4. ORTEP plot showing the twist-boat conformation of the six-membered ring in **2**.

Crystals were mounted in thin-walled glass capillaries, which were sealed. For **3** this measure was precautionary. For **1** and **2** it was required in order to maintain the integrity of the crystals.[23] Data were collected by using the θ–2θ scan mode, with $3° \leq 2\theta$ (Mo $K\bar{\alpha}$) $\leq 43°$ for **1** and **3** and $3° \leq 2\theta$ (Mo $K\bar{\alpha}$) $\leq 48°$ for **2**. The structures were solved by use of direct methods and difference Fourier techniques and were refined by full-matrix least-squares.[24a] Non-hydrogen atoms were refined anisotropically. Hydrogen atoms were included in the refinements as fixed isotropic scatterers (ideal positions or regularized difference Fourier positions for the xylyl methyl groups). Crystallographic data are summarized in Table I.[24b] All computations were performed on a Microvax II computer using the Enraf-Nonius SDP system of programs.

Results

The molecular geometry and the atom-labeling scheme for **1** are shown in the ORTEP plot of Figure 1. Selected atomic co-

---

(20) Arbuzov, A. E.; Zoroastrova, W. M. *Izv. Akad. Nauk SSSR, Otd. Khim. Nauk* **1953**, 453.

(21) Peake, S. C.; Fild, M.; Schmutzler, R.; Harris, R. K.; Nichols, J. M.; Rees, R. G. *J. Chem. Soc., Perkin Trans. 2* **1972**, 380.

(22) Sau, A. C.; Day, R. O.; Holmes, R. R. *Inorg. Chem.* **1981**, *20*, 3076.

(23) Crystals of **1** were of poor quality with etched surfaces, internal defects, and broad diffraction peaks. Crystals in an open container become cracked and opaque within 48 h. Crystals of **2** are deliquescent in an open container, puddling within 24 h.

(24) (a) The function minimized was $\sum w(|F_o| - |F_c|)^2$, where $w^{1/2} = 2F_oLp/\sigma_I$. (b) $R = \sum||F_o| - |F_c||/\sum|F_o|$ and $R_w = \{\sum w(|F_o| - |F_c|)^2/\sum w|F_o|^2\}^{1/2}$.

Table I. Crystallographic Data for Compounds 1–3

compd	**1**	**2**	**3**
formula	$C_{25}H_{19}O_4SF_{10}P$	$C_{23}H_{15}O_3S_2F_{10}P$	$C_{24}H_{21}O_3S_2P$
fw	636.44	624.44	452.52
cryst color	colorless	colorless	tan
dimens, mm	0.33 × 0.50 × 0.60	0.38 × 0.50 × 0.50	0.28 × 0.38 × 0.50
space group	$P\bar{1}$ (No. 2)	$P2_1/c$ (No. 14)	$P2_1/c$ (No. 14)
a, Å	11.239 (11)	14.485 (5)	13.493 (2)
b, Å	11.288 (5)	10.573 (4)	9.048 (3)
c, Å	11.934 (8)	16.626 (3)	18.149 (6)
α, deg	74.72 (5)		
β, deg	65.34 (6)	99.85 (2)	96.86 (2)
γ, deg	74.58 (6)		
V, Å^3	1306 (2)	2509 (2)	2200 (2)
Z	2	4	4
D_{calc}, g/cm^3	1.618	1.653	1.366
μ, cm^{-1}	2.783	3.629	3.256
relative trans coeff		0.9838–0.998	
no. of independ reflcns measd	2987 ($+h,\pm k,\pm l$)	3899 ($+h,+k,\pm l$)	2517 ($+h,+k,\pm l$)
no. of obsd reflcns $I \geq 3\sigma_I$	1925	2959	1609
$R(F)$	0.095	0.036	0.044
$R_w(F)$	0.127	0.049	0.056

Table II. Selected Atomic Coordinates and B_{equiv} Values in Crystalline $(Me_2C_3H_4O_2)P(OC_6F_5)_2(S\text{-}Xyl)$ (**1**)[a]

atom[b]	x	y	z	B_{equiv},[c] Å^2
S	0.9142 (3)	0.3088 (3)	0.6126 (3)	3.94 (7)
P	0.7352 (3)	0.2488 (2)	0.7260 (2)	3.06 (7)
O1	0.6700 (6)	0.3120 (6)	0.6249 (6)	3.6 (2)
O2	0.7172 (6)	0.1091 (6)	0.7455 (6)	3.4 (2)
O3	0.6154 (6)	0.3325 (6)	0.8273 (6)	3.5 (2)
O5	0.8175 (6)	0.1951 (6)	0.8339 (6)	3.4 (2)
C1	0.549 (1)	0.286 (1)	0.626 (1)	4.2 (3)
C2	0.604 (1)	0.076 (1)	0.7363 (9)	4.1 (3)
C3	0.569 (1)	0.147 (1)	0.625 (1)	4.0 (3)
C4	0.680 (1)	0.115 (1)	0.501 (1)	5.7 (4)
C5	0.439 (1)	0.114 (1)	0.637 (1)	5.6 (3)
C21	0.9127 (9)	0.3741 (9)	0.4611 (9)	3.5 (3)
C31	0.6085 (9)	0.3414 (9)	0.9423 (9)	3.2 (3)
C51	0.8776 (9)	0.0779 (8)	0.8634 (8)	3.0 (2)

[a] Numbers in parentheses are estimated standard deviations. [b] Atoms are labeled to agree with Figure 1. [c] Equivalent isotropic thermal parameters are calculated as $(4/3)[a^2\beta_{11} + b^2\beta_{22} + c^2\beta_{33} + ab(\cos\gamma)\beta_{12} + ac(\cos\beta)\beta_{13} + bc(\cos\alpha)\beta_{23}]$.

Table III. Selected Distances (Å) and Angles (deg) for $(Me_2C_3H_4O_2)P(OC_6F_5)_2(S\text{-}Xyl)$ (**1**)[a]

	Distances		
S–P	2.075 (4)	O2–C2	1.47 (2)
S–C21	1.77 (1)	O3–C31	1.37 (1)
P–O1	1.584 (8)	O5–C51	1.35 (1)
P–O2	1.588 (7)	C1–C3	1.53 (2)
P–O3	1.653 (6)	C2–C3	1.50 (2)
P–O5	1.779 (8)	C3–C4	1.55 (1)
O1–C1	1.46 (2)	C3–C5	1.54 (2)
	Angles		
P–S–C21	109.2 (4)	P–O2–C2	123.3 (6)
S–P–O1	93.1 (2)	P–O3–C31	127.1 (6)
S–P–O2	122.2 (2)	P–O5–C51	127.0 (7)
S–P–O3	121.4 (3)	O1–C1–C3	108.2 (8)
S–P–O5	81.4 (2)	O2–C2–C3	115.3 (8)
O1–P–O2	99.4 (4)	C1–C3–C2	108. (1)
O1–P–O3	90.1 (4)	C1–C3–C4	109.2 (8)
O1–P–O5	172.7 (4)	C1–C3–C5	109.6 (8)
O2–P–O3	114.7 (3)	C2–C3–C4	111.9 (8)
O2–P–O5	87.5 (4)	C2–C3–C5	109.3 (9)
O3–P–O5	88.9 (4)	C4–C3–C5	109. (1)
P–O1–C1	125.8 (6)		

[a] Estimated standard deviations in parentheses. The atom-labeling scheme is shown in Figure 1.

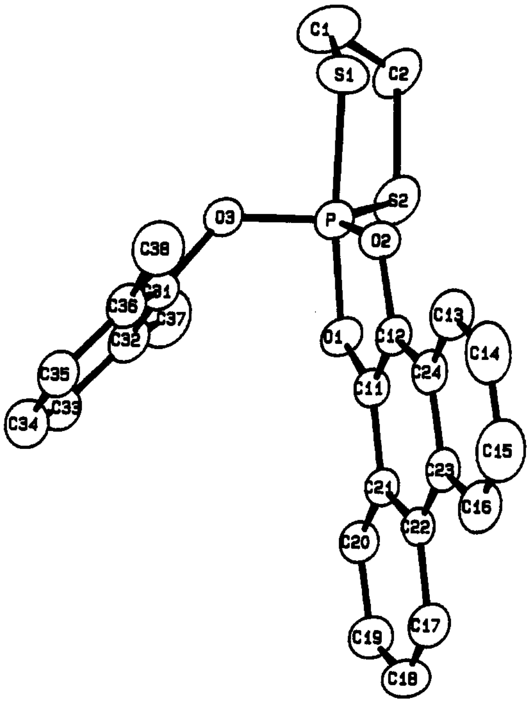

Figure 5. ORTEP plot of $(C_2H_4S_2)P(O_2C_{14}H_8)(O\text{-}Xyl)$ (**3**) with thermal ellipsoids at the 30% probability level. Hydrogen atoms are omitted for clarity.

Table IV. Selected Atomic Coordinates and B_{equiv} Values in Crystalline $(C_3H_6S_2)P(OC_6F_5)_2(O\text{-}Xyl)$ (**2**)[a]

atom[b]	x	y	z	B_{equiv},[c] Å^2
S1	0.05723 (5)	0.29611 (7)	0.82023 (4)	3.69 (1)
S2	0.08644 (5)	0.02131 (8)	0.90040 (5)	4.03 (2)
P	0.17009 (5)	0.16750 (7)	0.86735 (4)	2.92 (1)
O1	0.2610 (1)	0.0629 (2)	0.9005 (1)	3.35 (4)
O2	0.1969 (1)	0.1628 (2)	0.7753 (1)	3.46 (4)
O3	0.2243 (1)	0.2692 (2)	0.9301 (1)	3.42 (4)
C1	−0.0156 (2)	0.1849 (3)	0.7532 (2)	4.46 (7)
C3	−0.0778 (2)	0.1052 (3)	0.7983 (2)	5.07 (8)
C2	−0.0339 (2)	0.0783 (3)	0.8860 (2)	4.85 (7)
C11	0.3297 (2)	0.0773 (3)	0.9666 (2)	3.17 (5)
C21	0.2602 (2)	0.0873 (3)	0.7438 (2)	3.36 (6)
C31	0.1961 (2)	0.3922 (3)	0.9494 (2)	3.69 (6)

[a] Numbers in parentheses are estimated standard deviations. [b] Atoms are labeled to agree with Figure 3. [c] Equivalent isotropic thermal parameters are calculated as $(4/3)[a^2\beta_{11} + b^2\beta_{22} + c^2\beta_{33} + ab(\cos\gamma)\beta_{12} + ac(\cos\beta)\beta_{13} + bc(\cos\alpha)\beta_{23}]$.

ordinates and distances and angles for **1** are given in Tables II and III, respectively. The corresponding information for **2** and **3** is given in Figures 3 and 5 and in Tables IV–VII. For all three compounds, complete tabulations of atomic coordinates, anisotropic thermal parameters, distances and angles, and hydrogen atom parameters are provided as supplementary material.

Table V. Selected Distances (Å) and Angles (deg) for $(C_3H_6S_2)P(OC_6F_5)_2(O\text{-}Xyl)$ (**2**)[a]

	Distances		
S1–P	2.167 (1)	P–O3	1.606 (2)
S1–C1	1.827 (3)	O1–C11	1.359 (3)
S2–P	2.095 (1)	O2–C21	1.384 (3)
S2–C2	1.821 (3)	O3–C31	1.416 (3)
P–O1	1.736 (2)	C1–C3	1.522 (5)
P–O2	1.643 (2)	C3–C2	1.514 (5)
	Angles		
P–S1–C1	97.9 (1)	O1–P–O2	89.38 (9)
P–S2–C2	107.8 (1)	O1–P–O3	87.72 (9)
S1–P–S2	97.09 (4)	O2–P–O3	117.3 (1)
S1–P–O1	177.38 (7)	P–O1–C11	126.6 (2)
S1–P–O2	88.06 (7)	P–O2–C21	130.4 (2)
S1–P–O3	93.96 (7)	P–O3–C31	129.4 (2)
S2–P–O1	83.58 (7)	S1–C1–C3	112.6 (2)
S2–P–O2	117.49 (8)	C1–C3–C2	113.1 (2)
S2–P–O3	124.35 (8)	S2–C2–C3	115.1 (2)

[a] Estimated standard deviations in parentheses. The atom-labeling scheme is shown in Figure 3.

Table VI. Selected Atomic Coordinates and B_{equiv} Values in Crystalline $(C_2H_4S_2)P(O_2C_{14}H_8)(O\text{-}Xyl)$ (**3**)[a]

atom[b]	*x*	*y*	*z*	B_{equiv},[c] Å^2
S1	0.6194 (1)	0.3847 (2)	0.48176 (9)	6.65 (4)
S2	0.7990 (1)	0.4493 (2)	0.3919 (1)	6.42 (4)
P	0.71895 (9)	0.2617 (1)	0.41973 (7)	4.41 (3)
O1	0.8093 (2)	0.1663 (3)	0.3796 (2)	4.32 (7)
O2	0.7344 (2)	0.1524 (3)	0.4927 (2)	4.48 (7)
O3	0.6292 (2)	0.2128 (3)	0.3589 (2)	4.21 (7)
C1	0.6158 (5)	0.5456 (7)	0.4274 (5)	9.4 (2)
C2	0.7207 (4)	0.5987 (6)	0.4197 (4)	8.7 (2)
C11	0.8419 (3)	0.0466 (5)	0.4215 (2)	3.7 (1)
C12	0.8014 (3)	0.0374 (5)	0.4847 (3)	4.1 (1)
C31	0.6232 (3)	0.0895 (5)	0.3109 (2)	4.0 (1)

[a] Numbers in parentheses are estimated standard deviations. [b] Atoms are labeled to agree with Figure 5. [c] Equivalent isotropic thermal parameters are calculated as $(4/3)[a^2\beta_{11} + b^2\beta_{22} + c^2\beta_{33} + ab(\cos\gamma)\beta_{12} + ac(\cos\beta)\beta_{13} + bc(\cos\alpha)\beta_{23}]$.

Discussion

Synthesis. The monocyclic phosphoranes **1** and **2** were prepared by the oxidative addition of pentafluorophenol to the cyclic phosphite in diethyl ether solution in the presence of *N*-chlorodiisopropylamine, initially conducted at −78 °C and completed at room temperature. The reaction is illustrated in eq 1 for the formation of **1**. The overall yield of **1** was 57%, and that of **2**, 38%. The formation of **2** provides the first example of a monocyclic phosphorane containing a thiophosphorinane ring.

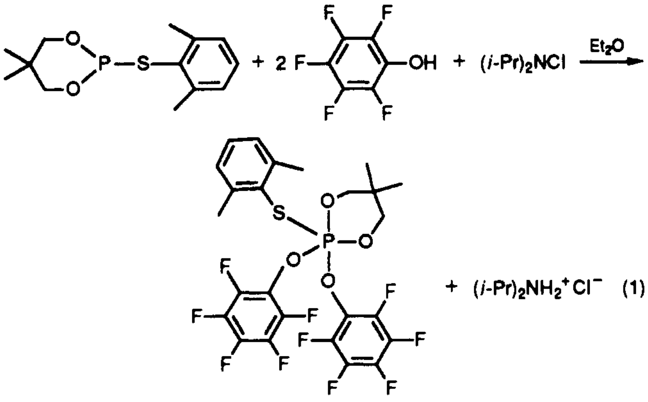

1

The spirocyclic derivative **3** was prepared neat by an oxidative addition of phenanthrenequinone to the cyclic thiophosphite **4** at 140 °C with a yield of 14%. All three represent new cyclic phosphoranes.

Table VII. Selected Distances (Å) and Angles (deg) for $(C_2H_4S_2)P(O_2C_{14}H_8)(O\text{-}Xyl)$ (**3**)[a]

	Distances		
S1–P	2.162 (2)	O1–C11	1.366 (5)
S1–C1	1.756 (7)	O2–C12	1.397 (5)
S2–P	2.105 (2)	O3–C31	1.411 (5)
S2–C2	1.823 (6)	C1–C2	1.517 (9)
P–O1	1.724 (3)	C11–C12	1.330 (6)
P–O2	1.646 (3)	C11–C21	1.434 (6)
P–O3	1.600 (3)	C12–C24	1.427 (6)
	Angles		
P–S1–C1	96.4 (3)	P–O1–C11	111.0 (3)
P–S2–C2	101.6 (2)	P–O2–C12	112.6 (3)
S1–P–S2	94.47 (8)	P–O3–C31	128.9 (3)
S1–P–O1	172.9 (1)	S1–C1–C2	110.5 (4)
S1–P–O2	85.2 (1)	S2–C2–C1	111.7 (4)
S1–P–O3	92.0 (1)	O1–C11–C12	113.1 (4)
S2–P–O1	83.9 (1)	O1–C11–C21	124.4 (4)
S2–P–O2	131.1 (1)	C12–C11–C21	122.5 (4)
S2–P–O3	115.1 (1)	O2–C12–C11	112.3 (4)
O1–P–O2	90.6 (2)	O2–C12–C24	123.6 (4)
O1–P–O3	94.9 (2)	C11–C12–C24	124.1 (4)
O2–P–O3	113.7 (2)		

[a] Estimated standard deviations in parentheses. The atom-labeling scheme is shown in Figure 5.

Structures. The structures of the sulfur-containing cyclic phosphoranes **1**–**3** show remarkable diversity, especially with regard to **1**. The geometry about the phosphorus atom for all three compounds is distorted trigonal bipyramidal (TBP) with the ring systems spanning axial–equatorial sites. In compound **1**, the six-membered ring has a chair conformation (Figure 2) that is somewhat flattened at the phosphorus end. For **2**, the thiophosphorinane ring has a twisted-boat conformation (Figure 4) with the axial sulfur atom at a tip of the boat. The sulfur-containing five-membered ring of **3** is best described as an envelope with the flap atom at C1 (Figure 5).

Previously, the only chair conformations found for phosphorinane rings in oxyphosphoranes were the oxaza systems A–C[4] cited in the Introduction where hydrogen bonding was proposed to exert a stabilizing influence. The present finding of this conformation in **1** is unique in its existence in the absence of hydrogen bonding. A further feature indicative of the extraordinary nature of **1** is that it provides the first example of a pentacoordinated phosphorus compound that has axial and equatorial bond lengths involving the same type of ligand that are the same, i.e., P–O1$_{ax}$ (1.584 (8) Å) and P–O2$_{eq}$ (1.588 (7) Å) are equal within experimental uncertainty. It is pointed out that the crystal structure was not of high quality. However, the comparative discussion of **1** and **2** to follow supports the signficance assigned to this structural determination. In addition to their apparent equality, these ring bond lengths show that the P–O1$_{ax}$ bond is the unusual one in that it is shorter than the average of this length (1.648 (4) Å) in other oxyphosphoranes containing similar phosphorinane rings by over 0.06 Å.[8,10] The equatorial bond length P–O2 is normal, being only about 0.01 Å shorter than the average value (1.598 (4) Å) for this class of substances. In the hydrogen-bonded oxyphosphoranes A–C[4] the related ring P–O axial bonds are of normal length varying from 1.65 to 1.67 Å and are longer than the corresponding ring P–O equatorial bonds by 0.062–0.084 Å.

Accompanying the unusually short P–O1$_{ax}$ bond length in **1**, the opposite P–O5$_{ax}$ bond attached to the C_6F_5 ring has a length that is very long, 1.779 (8) Å, compared to the average of 1.605 (3) Å for xylyloxy groups. Further, it exceeds the analogous P–O$_{ax}$ bond length in **2** (1.736 (2) Å) as well as the opposite P–O$_{ax}$ bond lengths in the hydrogen-bonded phosphoranes A–C,[4] whether they are in their boat or chair conformations. The latter values lie in the range of 1.71–1.74 Å. Both the P–O3$_{eq}$ bond length in **1** (1.653 (6) Å) and the P–O2$_{eq}$ bond length in **2** (1.643 (2) Å) that are connected to C_6F_5 rings are long as well. A bond length of 1.60–1.61 Å is typically observed for P–O$_{eq}$ bonds to xylyloxy groups.[8,10]

One is led to suggest that the acyclic OC_6F_5 groups in **1** and **2**, as a result of exerting a sizable electronegativity effect, supported to some extent by a steric interaction between neighboring OC_6F_5

Table VIII. Dihedral Angles between P–X_{eq}–C Planes and Equatorial Planes for Phosphoranes (deg)

	ring size, no. of atoms		
	5	6	acyclic group
1		54.6 (X = O)[a]	86.6 (S–Xyl), 85.1 (O–C_6F_5)
2		87.0 (X = S)[b]	89.6 (O–Xyl), 79.7 (O–C_6F_5)
3	82.4 (X = S) 88.2 (X = O)		71.4 (O–Xyl)
G[d]		56.1 (X = O)[c]	76.1 (O–Xyl), 88.5 (O–Xyl)

[a] Chair conformation. [b] Boat conformation. [c] Planar envelope ring conformation with P as the flap atom. [d] Reference 9.

groups, allow a more covalent P–O_{ax} bond to be formed to the phosphorinane ring system, which in turn stabilizes the chair conformation in **1**. The shortening of the P–$O1_{ax}$ bond length in **1** to the length of the P–O_{eq} bond accompanying increased covalency favors a chair in that maximum symmetry is achieved similar to that which is present for chair conformations occupying diequatorial positions in TBP geometries of anionic silicon compounds.[25] The boat conformation has the prow at the axial atom, O1 thus imparting a dissimilar character to P–O1 and P–O2. In the related thiophosphorinane ring system in **2**, the effects attributed to the pentafluorophenoxy ligand appear insufficient in the presence of the larger ring sulfur atoms and the boat conformation is present as usually found for saturated six-membered rings in TBP geometries.[4–10,18]

In contrast to **1**, the less electronegative sulfur atom has displaced an oxygen atom from an axial site in **2** similar to that previously found for D.[7] In we assume the apicophilicities of SR and OR are similar, as Trippett's[26] NMR work yielding activation energies for fluxional phosphoranes suggests, then ring strain relief acts as an overriding feature in locating sulfur-containing phosphorinane rings in axial–equatorial sites of a TBP instead of at the higher energy diequatorial positions. Related oxyphosphoranes E[10] and F,[10] which, like **2** and D,[7] have phosphorinane rings in boat conformations, exhibit different NMR behavior indicating that the S-xylyl group is more apicophilic than the O-xylyl group.

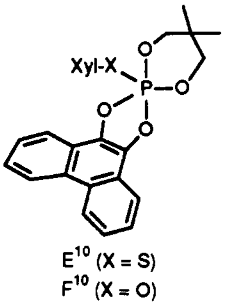

E[10] (X = S)
F[10] (X = O)

The fact that chair conformations for saturated six-membered rings are stabilized in axial–equatorial sites of a TBP in **1** and A–C[4] illustrates that a boat conformation is not a necessary requirement for the phosphorinane ring to be so located. Trippett[26] stated that the boat form was given preference in that it was the only one that allowed the lone pair of the equatorial ring heteroatom to reside in the equatorial plane.

As we have shown in earlier work, oxyphosphoranes possessing phosphorinane rings invariably position the rings in axial–equatorial sites of a TBP,[4–10,18] usually in a boat conformation, in preference to location of the rings at diequatorial sites. The closeness that the dihedral angle between the plane containing the ring atoms P–O_{eq}–C and the equatorial plane approaches 90° provides a measure to which Trippett's criterion[26] is met for boat conformations. A range of values from 76 to 86° for monocyclic[9] and spirocyclic[4,8,10] oxyphosphoranes with this type of ring shows that a considerable degree of back-bonding to phosphorus should result from this effect. However, we now know that nonboat conformations also form in axial–equatorial locations associated with the presence of hydrogen bonding in A–C[4] and electronegativity and steric effects in the case of **1**. Further, the axial–equatorial positioning of an unsaturated six-membered ring system in G,[9] where the ring is essentially planar other than the phosphorus flap atom, shows that, even in the absence of ligand influences or hydrogen bonding, nonboat forms locate in axial–equatorial sites of TBP.

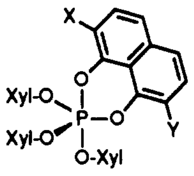

X = Y = H
X = Y = Cl
X = H, Y = Cl

G[9]

For comparison, the dihedral angles for **1**–**3** and G[9] are displayed in Table VIII and show that the less constrained acyclic oxy and thio ligands have dihedral angles that tend to approach 90°. This suggests that steric or intermolecular effects are not greatly inhibiting their orientation away from the "ideal" value. The dihedral angles for **1** and G,[9] involving six-membered rings in chair and envelope forms, respectively, have values near 55° as might be expected for nonboat ring arrangements. These values are considerably below the range cited for boat conformations, between 76 and 86°.[4,8–10]

It is interesting to note that, in contrast to five-coordinated phosphorus-containing phosphorinane rings where a boat conformation is normally observed, for four-coordinated phosphorus with these same rings, the chair conformation usually is the prevalent form.[27] On rare occasions, however, a boat conformation has been found to exist. For example, X-ray analysis of the 2,5-di-*tert*-butyl 2-oxo derivative revealed the first monocyclic boat form of this class, H.[28] There are two independent molecules in the unit cell. The two P–O ring bond lengths are equal, being 1.58 (3) Å in one independent molecule and 1.576 (4) Å in the other.[28]

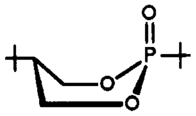

H

NMR and Intramolecular Ligand Exchange. The room-temperature ^1H NMR pattern of **1** indicating equivalence of the two phosphorinane ring methyl groups and equivalence of the four ring methylene protons as well as that of the two xylyloxy methyls suggests rapid ligand permutation where the ring in the TBP intermediate proposed for the ring interchange is confined to axial–equatorial sites. Accompanying this process, rapid C–O bond rotation of the xylyloxy methyl groups is indicated. Variable-temperature ^1H spectra of **1** in either CD_2Cl_2 or toluene-d_8 (Figure 6) indicate that pseudorotation is "stopped" at −60 °C. Consistent with a static structure, fourteen of the sixteen proton lines for **1** in $CDCl_3$ solution are resolved in the CH_2 region for the six-membered ring. Fifteen lines are present in this region in toluene solution. Sixteen lines are expected for the presence of four different methylene protons, i.e., four ABX quartets (where X = P). Accompanying this change, two phosphorinane ring methyl signals and two xylyloxy methyl signals emerge. Thus, the low-temperature NMR data support a solution-state structure that has the same ring placement as found in the X-ray structure.

The assignment of the ^1H NMR spectrum of **2** at 20 °C is assisted by comparison to that of D.[7] The presence of a doublet of triplets in the SCH_2 region and one quintet in the CH_2–CH_2

---

(25) Day, R. O.; Sreelatha, C.; Deiters, J. A.; Johnson, S. E.; Holmes, J. M.; Howe, L.; Holmes, R. R. *Organometallics* **1991**, *10*, 1758.

(26) Trippett, S. *Pure Appl. Chem.* **1974**, *40*, 595.

(27) Maryanoff, B. E.; Hutchins, R. O.; Maryanoff, C. A. *Top. Stereochem.* **1979**, *11*, 187 and references cited therein.

(28) Day, R. O.; Bentrude, W. G.; Yee, K. C.; Setzer, W. N.; Deiters, J. A.; Holmes, R. R. *J. Am. Chem. Soc.* **1984**, *106*, 103.

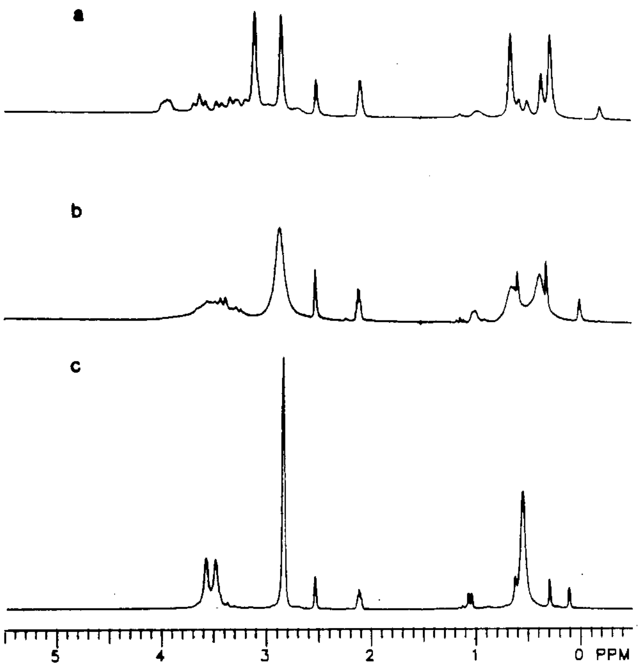

Figure 6. Partial ^1H NMR spectra of **1** in toluene-d_8 as a function of temperature: (a) −60 °C; (b) −20 °C; (c) 16 °C. Low-intensity impurity peaks are present in (c) at 0.1, 0.3, 1.05, 2.13, and 2.53 ppm.

region of the six-membered sulfur-containing ring (Figure 7a) is consistent with equivalence of all four SCH_2 protons and equivalence of the two CH_2CH_2 protons. The separation of the two triplets gives $^3J_{P-SCH_2}$ = 31 Hz, which compares with $^3J_{P-SCH_2}$ values found for D of 35.4 and 25.2 Hz.[7] Coupled with the singlet assigned to the xylyloxy methyl protons, a nonrigid molecule is indicated undergoing pseudorotation by a simple Berry process involving axial–equatorial ring interchange, similar to that for **1** with accompanying rapid C–O bond rotation of the xylyloxy methyl groups.

While the ^1H NMR pattern of **2** by itself does not establish an axial–equatorial ring arrangement (it is also in agreement with a static structure having a diequatorial ring arrangement[7]), more extensive NMR data on related phosphoranes containing six-membered rings, both monocyclic[9] and spirocyclic,[4,8,10] are uniquely interpreted in terms of axial–equatorial ring placement in a trigonal-bipyramidal geometry. The close similarity in the X-ray structure between **1** and **2** and the fact that the similar a-e $\rightleftharpoons$ e-a pseudorotational process in **1** resulted in a ^1H NMR pattern for a static structure in agreement with the solid-state structure suggests that this would also occur for **2**. The ready decomposition of **2** prevented a variable-temperature study similar to that performed for **1**.

The ^1H NMR spectrum of **3** (Figure 7b) is invariant over the range 20 to −20 °C. The presence of only one singlet in the xylyloxy methyl group region and one doublet due to phosphorus coupling assignable to the protons of the methylene groups suggests a nonrigid structure undergoing rapid pseudorotation over this temperature range. Ligand exchange via diequatorial placement of the phenanthrene ring in a TBP intermediate accompanied by rapid C–O bond rotation of the xylyloxy group allows equivalence of all four ring methylene protons and brings about equivalence of the two xylyloxy methyl groups. The only other spirocyclic phosphorane with a phenanthrene ring that exhibits this type of ligand exchange, i.e., (a-e) $\rightleftharpoons$ (e-e), is E.[10] However, unlike **3**, on lowering of the temperature below 0 °C, this exchange "stops". At present, we have no explanation for the low barrier implied for this exchange process for **3**.

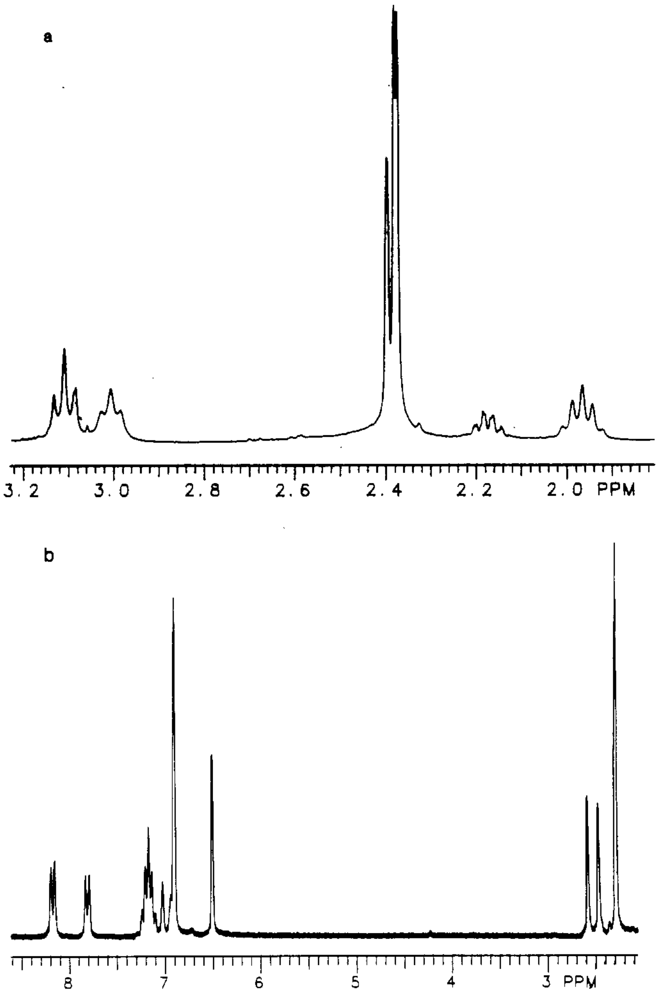

Figure 7. ^1H NMR spectra at 20 °C of (a) **2** in $CDCl_3$ and (b) **3** in toluene-d_8. A toluene signal is present in (b) at 6.9 ppm.

The activation energy for pseudorotation of **1** involving a-e $\rightleftharpoons$ e-a ring interchange via TBP intermediates of the type shown in Scheme I was calculated as 12.6 kcal/mol from eq 2[29] with the insertion of the line separation at −70 °C ($\Delta\nu$ = 77.3 Hz) and coalescence temperature (T_c = 263.2 K) for the temperature-dependent ^1H spectra in toluene of resonances assigned to the methyl groups of the six-membered rings (Figure 6). From the coalescence temperature (T_c = 238.16 K) and the line separation at −70 °C ($\Delta\nu$ = 51.9 Hz) for the methyl resonances of the S-xylyl group, ΔG^* of 11.6 kcal/mol resulted. These values are not significantly different from each other considering an approximate uncertainty of 0.5–1.0 kcal/mol associated with the application of eq 2.[29] Hence we might view the slowing down of the pseudorotation process (Scheme I) to be concerted with the inhibition of C–O bond rotation of the xylyl group.

$$\Delta G^* = 4.57 \times 10^{-3}\ T_c\left(10.32 + \log\left(T_c\sqrt{2}/\pi\Delta\nu\right)\right) \quad (2)$$

Other monocyclic[9] oxyphosphoranes containing phosphorinane rings that we have studied show similar exchange behavior. In particular, variable-temperature ^1H NMR spectra of I support pseudorotation involving axial–equatorial ring interchange at room temperature, which is inhibited at low temperature.[9] Here the saturated six-membered ring is in a twist-boat conformation rather

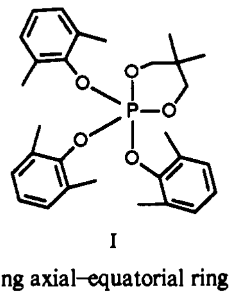

I

---

[29] (a) Kessler, H. *Angew Chem.* **1970**, *82*, 237. (b) See also: Buono, G.; Llinas, J. R. *J. Am. Chem. Soc.* **1981**, *103*, 4532.

Scheme I

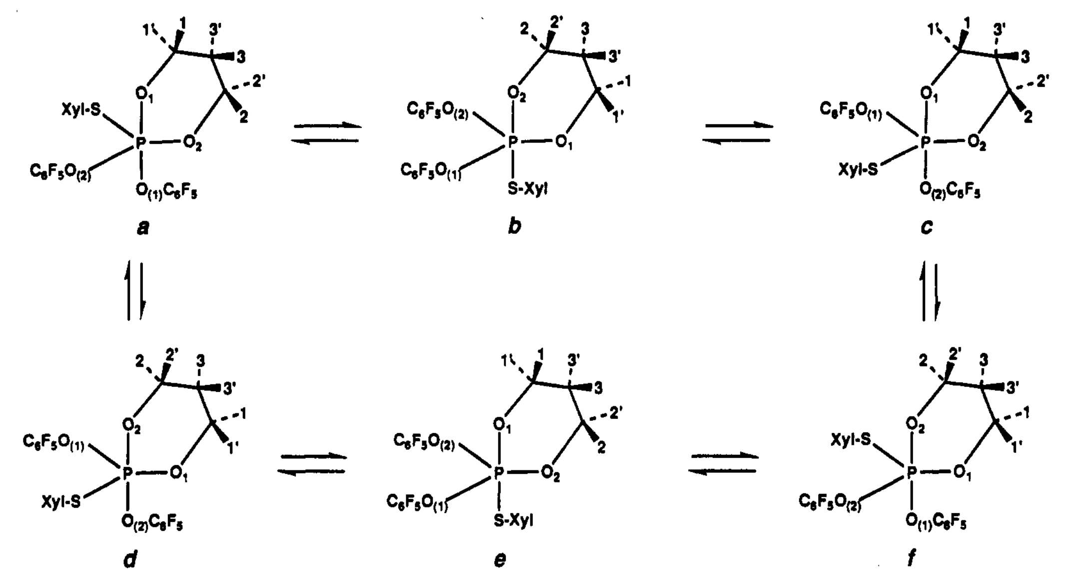

than the chair found for **1**. The activation energy for a-e ⇌ e-a pseudorotation is the same, 10.6 ± 0.1 kcal/mol, whether the signals being monitored emanate from the xylyloxy ring protons, the xylyloxy methyl protons, the phosphorinane methylene protons, or the phosphorinane methyl protons.

Steric hindrance in reaching a square-pyramidal transition state for I was advanced[9] to account for the cessation of simple Berry pseudorotation at −68 °C (similar to that in Scheme I) compared to that encountered in related spirocyclic phosphoranes J[8,30] and K,[30] where axial–equatorial ring exchange is not stopped at this temperature. In the acyclic derivative MeP(OXyl)$_4$, Westheimer[31] reasoned that severe steric crowding was present due to the interaction of the four xylyloxy groups. Normally this class of phosphoranes undergoes ligand exchange uninhibited at −65 °C. Since the activation energy was 7.7 kcal/mol, i.e., less than that found for I,[9] the degree of steric effect in the latter compound was placed quantitatively higher. In view of the closeness in ΔG^{*} values for **1** and I for this same type of exchange, a comparable steric effect suggests itself. However, there are several obvious differences between these two molecules, all of which may enter in in establishing a barrier energy for pseudorotation. For **1**, the highest energy transition state under Scheme I most likely is a square pyramid of the type g. This closely resembles the likely transition state (h) in the related exchange process for I. The ring conformation, which is a chair in **1** and a boat in I, most likely is a chair in both g and h. Hence, all that one reasonably can say is that a steric effect is likely present in **1** but its relative magnitude is undefined.

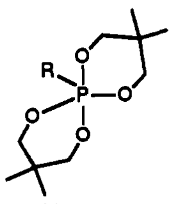

J[8,30] (R = Ph)
K[30] (R = Me)

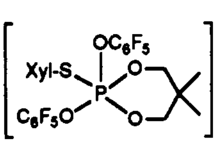

g

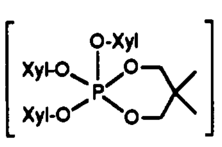

h

Structural Details. For the chair conformation in **1** (Figure 2), the atoms O1, O2, C1, and C2 are coplanar to within ±0.036 Å, with atoms P and C3 displaced from this plane in opposite directions by distances of 0.507 and 0.683 Å, respectively. The twisted-boat conformation found for **2** (Figure 4) has the atoms P, S2, C1, and C3 coplanar only to within ±0.145 Å (reflecting the twist), with atoms S1 and C2 displaced from this plane in the same direction by distances of 1.048 and 0.753 Å, respectively.

The atoms of the equatorial plane (P, O2, O3, and S2) are coplanar to within ±0.050 Å. For purposes of comparison to **3** it is interesting to note that the ring atoms P, S1, S2, and C2 define a plane (±0.052 Å) that is nearly perpendicular to the equatorial plane (dihedral angle of 88.7°).

In the chair ring system of **1**, the corresponding atoms P, O1, O2, and C2 are not coplanar. Rather, C2 is displaced a distance of 0.666 Å from the plane defined by the other three atoms. This plane is nearly perpendicular to the equatorial plane (atoms P, O2, O3, and S coplanar to within ±0.066 Å) with which it makes a dihedral angle of 87.3°. By contrast, the dihedral angle between the plane defined by atoms P, O2, and C2 and the equatorial plane is 54.6°.

In compound **3**, the five-membered sulfur-containing unsaturated ring has atoms P, S1, S2, and C2 that are coplanar to within ±0.092 Å and has C1 displaced from this plane by a distance of 0.728 Å. As in the case of **2**, this plane is nearly perpendicular to the equatorial plane (P, O2, O3, and S2 coplanar to within ±0.009 Å). In this case the dihedral angle is 89.2°.

The entire 17 atom fragment comprised of the phenanthrene moiety, O1, O2, and P for **3** is coplanar to within ±0.036 Å. The dihedral angle between this plane and the equatorial plane is 86.0°. For **3**, distortions away from the ideal TBP geometry follow the Berry pseudorotation coordinate[32] connecting the TBP with S1 and O1 axial to a rectangular pyramid (RP) with the acyclic O3 in the apical position. By use of the dihedral angle method[33] with unit vectors, the geometry is displaced 28.2% from the TBP toward the RP.

Distortions for **1** and **2** from the ideal TBP do not follow the Berry pseudorotation coordinate. For **1**, the distortion is "anti-Berry" in nature: The closing down of the equatorial angle O2–P–O3 to 114.7 (3)° is accompanied by a closing down of the axial angle to 172.7 (4)°, where the axial atoms O1 and O5 are tipped toward the equatorial sulfur atom. For **2**, while the equatorial

---

(30) Chang, B. C.; Conrad, W. E.; Denney, D. B.; Denney, D. Z.; Edelman, R.; Powell, R. L.; White, D. W. *J. Am. Chem. Soc.* **1971**, *93*, 4004.

(31) Szele, I.; Kubisen, S. J., Jr.; Westheimer, F. H. *J. Am. Chem. Soc.* **1976**, *98*, 3533.

(32) Berry, R. S. *J. Chem. Phys.* **1960**, *32*, 933.

(33) Holmes, R. R.; Deiters, J. A. *J. Am. Chem. Soc.* **1977**, *99*, 3318.

angle S2–P–O3 is opened up to 124.35 (8)°, the axial atoms are tipped away from these atoms toward O2 for an angle S1–P–O1 of 177.38°.

Conclusion. With regard to ring orientation, the study of new oxyphosphoranes possessing sulfur rings and pentafluorophenoxy ligands leads to axial–equatorial ring placement in TBP geometries similar to that found in other studies with cyclic pentaoxyphosphoranes.[4–10,18] Thus far, use of electronegative ligands, steric and hydrogen bonding[4] effects, introduction of trans-fused rings,[10] or varying ring size from five- to eight-membered[8,9] has not yielded a solid-state structure of a pentacoordinated phosphorus molecule displaying diequatorial ring occupancy. However, use of these variations has led to the formation of chair conformations[4] in addition to the more prevalent boat form[7–10] for phosphorinane rings in axial–equatorial sites of TBP geometries. In the present study, the unique chair conformation found for the six-membered ring of **1** had a short P–O axial bond equal in length to the P–O equatorial bond within the accuracy of the measurement, the first observation of this kind in pentacoordinated phosphorus chemistry. Future work on structural preferences of cyclic oxyphosphoranes should prove valuable in assisting mechanistic studies of *c*-AMP action and more generally in interpreting mechanisms of reaction of cyclic phosphates.

Acknowledgment. The support of this research by the National Science Foundation (Grant CHE 88-19152) and the Army Research Office is gratefully acknowledged.

Supplementary Material Available: Tables of atomic coordinates, thermal parameters, additional bond lengths and angles, and hydrogen atom parameters (Tables S1–S4 for **1**, Tables S5–S8 for **2**, and Tables S9–S12 for **3**) (24 pages); listings of observed and calculated structure factors for **1**–**3** (28 pages). Ordering information is given on any current masthead page.

Contribution from the Department of Chemistry,
Wayne State University, Detroit, Michigan 48202

Stereochemical Perturbations of the Relaxation Behavior of (^{2}E)Cr(III). Ground-State X-ray Crystal Structure, Photophysics, and Molecular Mechanics Simulations of the Quasi-Cage Complex [4,4′,4″-Ethylidynetris(3-azabutan-1-amine)]chromium Tribromide[1]

Marc W. Perkovic, Mary Jane Heeg, and John F. Endicott*

Received September 18, 1990

The X-ray crystal structure of $Cr(sen)^{3+}$ (sen = 4,4′,4″-ethylidynetris(3-azabutan-1-amine)) demonstrates that the coordination environments are very similar in this complex and $Cr(en)_3{}^{3+}$. However, the photophysical behaviors of these complexes contrast markedly, with $Cr(sen)^{3+}$ having a much shorter ^{2}E excited-state lifetime (by a factor of at least 10^4) in ambient fluid solutions. The bond angles of the neopentyl cap (N–C–C and CH_2–C–CH_2) of $Cr(sen)^{3+}$ are 5–10° larger than normal, and this is attributed to trigonal strain in the ligand induced by coordination to Cr(III). MM2 calculations indicate that coordination geometry preferred by the ligand would be very nearly halfway between the ideal prismatic and antiprismatic microsymmetries. In contrast to the fluid solution behavior, (^{2}E)$Cr(sen)^{3+}$ doped into $[Rh(sen)](ClO_4)_3$ was found to have a 13-μs lifetime at 298 K. The facile, thermally activated fluid solution excited-state relaxation channel is attributed to a large amplitude ligand-promoted trigonal twist of the electronically excited complex. $[Cr(sen)]Br_3$, $CrN_6C_{11}H_{30}Br_3$, crystallizes in the monoclinic space group $P2_1/c$ with $Z = 4$ and $a = 13.964$ (4) Å, $b = 10.777$ (2) Å, $c = 13.027$ (3) Å, and $\beta = 98.34$ (2)°. The structure refined to $R = 0.055$ and $R_w = 0.050$ with 1612 observed reflections.

Introduction

Transition-metal excited states have considerable potential for use as chemical reagents or as key elements in optoelectronic systems.[2–4] Realization of this potential often requires that excited-state electronic configurations persist for appreciable time periods when the conditions are ambient or nearly ambient. However, the ambient lifetimes of transition-metal excited states are usually dictated by poorly understood thermal deactivation processes. Chromium(III) complexes nicely illustrate the problems involved, since the decay of the lowest energy excited state, (^{2}E)Cr(III), is spin forbidden and does not involve a change of orbital electronic population. As a consequence, the ^{2}E excited state and the $^4A_2$ ground state have very nearly identical molecular geometries, and the excited-state lifetime should be dictated by nearly temperature-independent tunneling processes.[5,6] Yet (^{2}E)Cr(III) excited-state lifetimes are usually strongly temperature dependent in ambient fluid solutions and lifetimes in the subnanosecond regime are not uncommon.[5] The observed relaxation behavior can be represented as

$$\tau^{-1} = k = k_{\text{lim}} + k(T) \qquad (1)$$

where τ is the observed mean lifetime,[7,8] k_{lim} is the limiting low-temperature (nearly temperature independent) relaxation rate constant, and $k(T)$ represents the thermally activated relaxation behavior. For (^{2}E)Cr(III) excited-state decay, $k(T)$ has been found to increase monotonically with temperature[5] and it is often fitted to a simple Arrhenius function, $k(T) = A \exp(-E_a/RT)$.[9,10] This behavior is suggestive of simple chemical reactions in which a reactant must acquire thermal energy sufficient to allow the changes in molecular geometry (including necessary changes in position of solvent, as well as reactant nuclei) necessary to generate the transition-state characteristic of the reaction process.[5a] However, there are usually several possible, perhaps competing, pathways for the thermally activated decay of electronically excited molecules.[5a,8,10] Thus, for Cr(III) complexes several distinct

---

(1) We gratefully acknowledge the Division of Chemical Sciences, Office of Energy Research, U.S. Department of Energy for partial support of this research.

(2) Balzani, V.; Moggi, L. *Coord. Chem. Rev.* **1990**, *97*, 313.

(3) Hopfield, J. J.; Onuchic, J. N.; Beratan, D. N. *J. Phys. Chem.* **1989**, *93*, 6350.

(4) Gütlich, P.; Hauser, A. *Coord. Chem. Rev.* **1990**, *97*, 1.

(5) For reviews, see: (a) Endicott, J. F.; Ramasami, T.; Tamilarasan, R.; Lessard, R.; Ryu, C. K.; Brubaker, G. R. *Coord. Chem. Rev.* **1987**, *77*, 1–87. (b) Forster, L. S. *Chem. Rev.* **1990**, *90*.

(6) Important features of (^{2}E)Cr(III) excited-state relaxation in the low-temperature regime (k_{lim}) are examined in detail elsewhere: (a) Ryu, C. K.; Lessard, R. B.; Lynch, D.; Endicott, J. F. *J. Phys. Chem.* **1989**, *93*, 1752. (b) Endicott, J. F.; Lessard, R. B.; Lynch, D. L.; Perkovic, M. W.; Ryu, C. K. *Coord. Chem. Rev.* **1990**, *97*, 65.

(7) The (^{2}E)Cr(III) decays have often been observed to be biexponential,[5b,8] so eq 1 should be regarded as somewhat idealized. The fluid solution lifetimes of the complexes reported in this paper fit single exponential behavior reasonably well.

(8) Forster, L. S.; Murrow, D.; Fucaloro, A. F. *Inorg. Chem.* **1990**, *29*, 3706.

(9) Non-Arrhenius behavior has sometimes been observed,[5] and it has also been suggested that $k(T)$ might approach a high-temperature-limiting value for some complexes.[10]

(10) Lessard, R. B.; Endicott, J. F.; Perkovic, M. W.; Ochromowycz, L. M. *Inorg. Chem.* **1989**, *28*, 2574.

0020-1669/91/1330-3140$02.50/0